

RESEARCH

Open Access



Temperature-dependent shifts in gut microbiota and metabolome of olive flounder (*Paralichthys olivaceus*): implications for cold-water aquaculture expansion and probiotic applications

Che-Chun Chen^{1,2}, Yu-Ping Chen³, Hsiao-Tsu Yang¹, Yu-Ling Chen¹, Chen-Wei Wu¹, Hong-Yi Gong^{4,5}, Yuan-Shing Ho³ and Ying-Ning Ho^{1,2,5*}

Abstract

Background In recent years, rising temperatures due to climate change have become significant stressors in aquatic environments, impacting disease incidence, growth, and gut microbiota in fish. Cold-water species, such as the olive flounder (*Paralichthys olivaceus*), are particularly vulnerable to increasing water temperatures. Despite its economic importance as a species farmed in East Asia, research on temperature-dependent shifts in the gut microbiota and metabolome of olive flounder remains limited. This study investigates the effects of water temperature on the gut microbiota and metabolome of olive flounder using full-length 16 S rRNA sequencing with Oxford Nanopore Technologies and metabolomics analysis with high-resolution liquid chromatography-mass spectrometry (LC-MS). The analysis compares individuals exposed to three water temperatures (18 °C, 22 °C, and 26 °C).

Results Temperature significantly influenced the composition of gut microbiota, with an increase in Gammaproteobacteria abundance at higher temperatures. Potential pathogens such as *Vibrio* and *Photobacterium* increased from 22 °C to 26 °C, while *Pseudomonas* declined, suggesting an elevated risk of pathogen infection at 26 °C. Functional predictions revealed that gut bacteria regulated host metabolism, particularly carbohydrate, amino acid, and lipid pathways. Metabolomic analysis showed reduced levels of polyunsaturated fatty acids (PUFAs) and phosphatidylcholine (PC)-related metabolites at higher temperatures. Notably, the umami flavor-related compound aspartic acid decreased, while the bitter flavor-related compound phenylalanine increased. Correlation analysis identified significant associations between bacterial genera, such as *Comamonas*, *Pseudomonas*, *Sphingomonas*, and *Stentotrophomonas* (positive correlation), and *Legionella* and *Phaeobacter* (negative correlation), with shifts in PUFAs and PC metabolites.

*Correspondence:

Ying-Ning Ho
ynho@mail.ntou.edu.tw

Full list of author information is available at the end of the article



© The Author(s) 2025. **Open Access** This article is licensed under a Creative Commons Attribution-NonCommercial-NoDerivatives 4.0 International License, which permits any non-commercial use, sharing, distribution and reproduction in any medium or format, as long as you give appropriate credit to the original author(s) and the source, provide a link to the Creative Commons licence, and indicate if you modified the licensed material. You do not have permission under this licence to share adapted material derived from this article or parts of it. The images or other third party material in this article are included in the article's Creative Commons licence, unless indicated otherwise in a credit line to the material. If material is not included in the article's Creative Commons licence and your intended use is not permitted by statutory regulation or exceeds the permitted use, you will need to obtain permission directly from the copyright holder. To view a copy of this licence, visit <http://creativecommons.org/licenses/by-nc-nd/4.0/>.

Conclusions This study demonstrates that environmental temperature significantly affects the gut microbiota and muscle metabolites of olive flounder. Higher temperatures diversified gut bacterial communities and altered metabolite profiles, with reductions in PUFAs and PC-related compounds linked to specific bacterial genera. These findings highlight the potential of these bacterial genera as biomarkers or probiotics for improving aquaculture practices and environmental adaptation strategies. By establishing a strong correlation between gut microbiota and muscle metabolites, this research provides insights that could contribute to sustainable flounder farming and enhance resilience to climate change.

Keywords Olive flounder, Cold-water species, Gut microbiota, Metabolomics, Oxford nanopore technologies

Backgrounds

In recent years, rising temperatures due to climate change have caused significant environmental changes, creating temperature stress for many aquatic species. Water temperature is a critical factor influencing fish feeding, growth [1], and immune responses [2]. For cold-water species such as the olive flounder (*Paralichthys olivaceus*), an economically important aquaculture species in China, Korea, and Japan [3], temperature fluctuations pose serious challenges. According to the Food and Agriculture Organization of the United Nations (FAO), global aquaculture production of olive flounder reached approximately 46,413 tons in 2020 [4]. The species thrives within an optimal temperature range of 15–20 °C [5], making it highly susceptible to the impacts of rising global temperatures. A comprehensive scientific understanding of how elevated water temperatures affect olive flounder is crucial for mitigating these challenges and ensuring sustainable aquaculture practices.

Higher temperatures negatively impact aquaculture species by reducing growth, increasing mortality, and disrupting reproduction. They also influence gut microbiota, disease resistance, and metabolism [6]. The gut microbiota plays a crucial role in host nutrition, development, immunity, and resilience to environmental stressors [7]. Additionally, recent research has shown that temperature changes not only influence the endogenous compounds in fish but also affect the biochemical composition of fish fillets [6]. For example, thermal conditions in the cultivation environment influence the fatty acid profile, particularly the n-3 fatty acid content, as observed in carp [8], rainbow trout [9], and European bass [10]. Similarly, studies on Japanese flounder have shown that higher temperatures lead to lower lipid content [11, 12].

In aquaculture species, dietary components, environmental stressors, and microbial activity in the gut can impact muscle composition and quality by modulating metabolic pathways related to lipid metabolism, amino acid utilization, and energy balance. However, there is limited knowledge about how temperature-driven shifts in gut microbiota affect metabolites in olive flounder, leaving a critical gap in understanding the interactions between microbiota and host metabolism under changing environmental conditions. To address this gap,

advanced sequencing and metabolomics techniques offer valuable tools. Oxford Nanopore Technologies (ONT) MinION™ sequencing, which targets the full-length 16 S rRNA gene, enables sensitive and high-resolution identification of bacterial communities in environmental and aquaculture systems [13]. The technique's ability to generate long reads improves species-level resolution and enhances the accuracy of microbial community profiling [14–16]. Metabolomics, leveraging high-resolution mass spectrometry (HR-MS) coupled with liquid chromatography (LC), has proven indispensable for analyzing metabolites and identifying novel biomarkers [17, 18]. This approach has been used to assess the metabolic responses of fish to various stressors, including sewage pollution [19], hypoxia [20], and temperature fluctuations [21].

Despite the significant role of gut microbiota and metabolites in fish health, the effects of temperature on these factors in cold-water olive flounder (*P. olivaceus*) remain poorly understood. By integrating muscle metabolome analysis with gut microbiota profiling, our study aims to provide a comprehensive view of how environmental factors, such as temperature, may induce systemic metabolic shifts that ultimately impact muscle quality. This holistic approach not only enhances our understanding of host–microbiome interactions but also supports the development of targeted nutritional and management strategies in aquaculture.

Materials and methods

Sample collection

The flounder samples used in this study were collected from the Eastern Marine Biology Research Center, Fisheries Research Institute, Ministry of Agriculture, Taitung, Taiwan. Fish were reared in 0.5-ton FRP tanks under different temperature conditions. We used a combination of deep and surface water, along with a heater, to maintain temperatures at 18 °C, 22 °C, and 26 °C. After 60 days of cultivation, samples were collected. The average body weights of the fish were 97.03 ± 4.63 g (18 °C), 97.95 ± 9.62 g (22 °C), and 92.28 ± 5.93 g (26 °C). Each treatment group consisted of 15 fish, five healthy individuals of each group (18 °C, 22 °C, and 26 °C) were randomly harvested for the collection of gut samples.

The intestinal tissues were dissected with sterilized scissors and tweezers, and complete intestinal tissues were transferred to sterilized petri dishes. Then washed with 200 μ L of sterilized 1 \times PBS, and the midgut and hindgut were ground and weighed in sterilized 1.5 mL Eppendorf and 400 μ L of DNA/RNA Shield Reagent (Zymo Research Corporation, USA) was added immediately. We used the entire midgut and hindgut of *P. olivaceus* for microbial community analyzing. This approach was chosen to provide a comprehensive overview of the microbiota composition under different temperature

conditions. An illustrative abstract of the processes and software utilized is depicted in Fig. 1.

DNA extraction and 16 S rRNA gene amplification

Fish gut microbiome DNA was extracted using a Quick-DNA[™] HMW MagBead Kit (Zymo Research Corporation, USA) according to manufacturer’s protocol. Q5[®] High-Fidelity DNA Polymerase (New England Biolabs, UK) and universal primers 27F and 1492R (27F: 5'-AGA GTT GAT CCT GGC TCA G; 1492R: 5'-GGT TAC CTT G TTAC GACTT) were used for the polymerase chain reaction (PCR) to amplify 16S rRNA. PCR barcode sequences

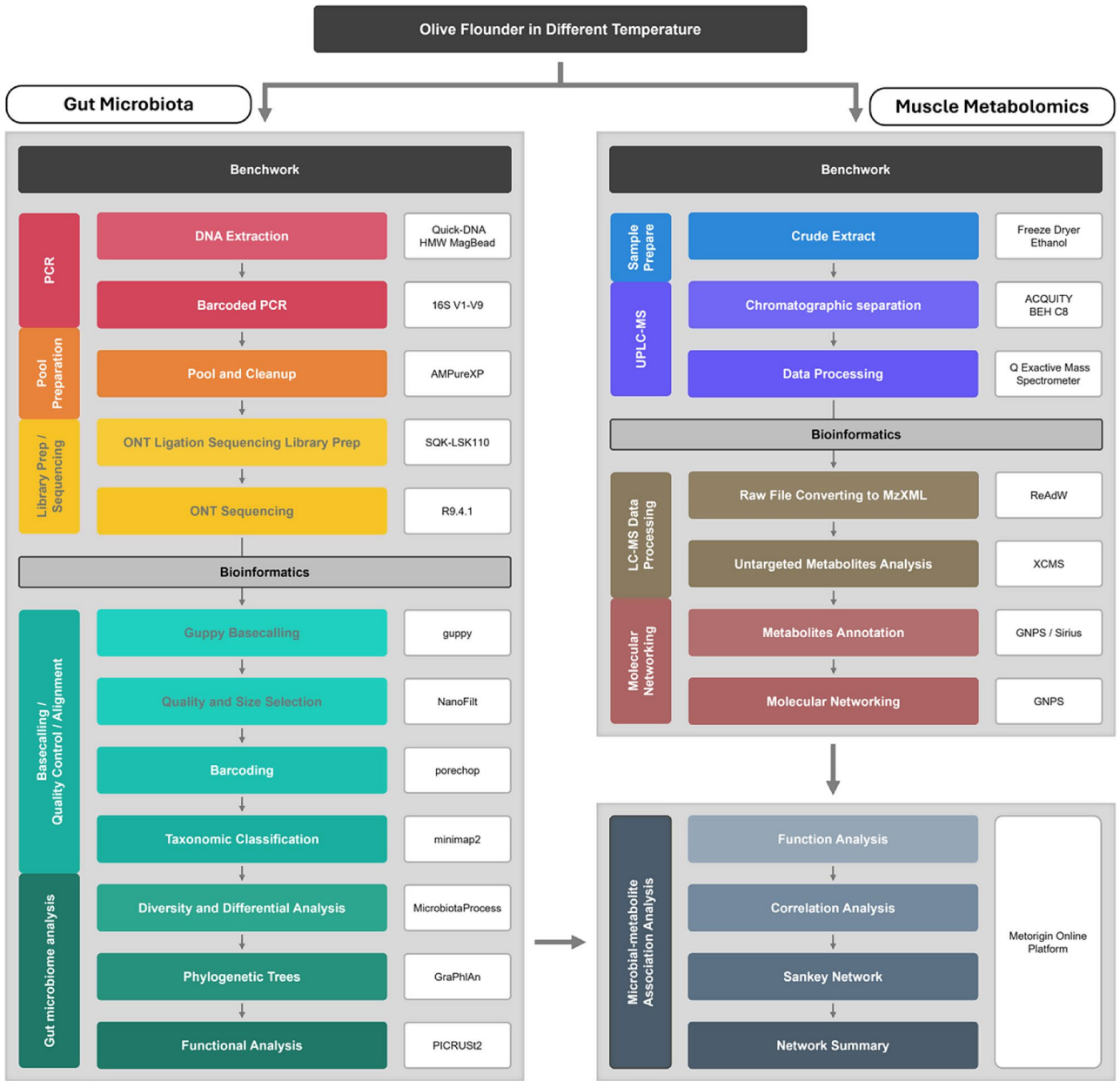


Fig. 1 Experimental design and workflow for studying olive flounder under different temperature conditions. The experiment is divided into three main components: gut microbiota analysis, muscle metabolomics, and their association analysis

(length: 24 bp) provided by Oxford (Oxford Nanopore Technologies, UK) were added to the 5' cap of the universal primers prior to amplification. The amplified region of 16 S rRNA was V1 to V9 (full length: ~1.5 kbp) and the PCR products were confirmed by electrophoresis. PCR products were then purified using the AMPure XP Purification Kit (Beckman Coulter, USA) to remove interfering substances. The DNA concentration of all purified samples was measured using a Qubit 4 Fluorometer (Thermo Fisher Scientific, USA). After quantification, the amplicons from all barcode PCR reactions were adjusted to the same concentration based on the Qubit measurements and then pooled into a single tube for subsequent library preparation.

Oxford nanopore technologies library Preparation and data processing

Library preparation was performed using the SQK-LSK109 kit (Oxford Nanopore Technologies, UK) following the manufacturer's instructions. The total DNA was loaded onto a MinION using a FLO-MIN106 Flow Cell (R9.4.1) and sequenced for 96 h using MinKNOW software (version 20.10.3). The fast5 file was then converted using the basecaller Guppy (version 4.2.2, https://github.com/timkahlke/LongRead_tutorials). NanoFilt (version 2.8.0) [22] was used to filter fastq files for sequences smaller than 1450 bp, larger than 1650 bp and with Q values less than 10 to remove non-target amplicons and sequences of poor sequencing quality. Sequences were then sorted using Porechop (version 0.2.4, <https://github.com/rrwick/porechop>) and adapters removed. Minimap2 (version 1.2.0) [23] was used for data alignment and microbial species taxonomy, and Pavian (version 1.2.0) [24] was used for data comparison analysis. The database of 16 S rRNA sequences was obtained from the National Center for Biotechnology Information (NCBI) (released on 17th February 2022).

Gut Microbiome analysis

The R programming language (version 4.1.3) was used to analyze the gut microbiome. The rarefy function in the vegan package was used to calibrate all samples to the minimum number of reads in order to have the same number of reads for all samples. Rarefied reads were used to calculate the alpha diversity indices and assess the variation in bacterial community composition among different groups. The alpha diversity of all samples, including diversity, richness and evenness indices (Chao1, Shannon, and Pielou's index) were then calculated using the MicrobiotaProcess package [25]. ANOVA was used to calculate the variability in richness and diversity between samples. Bray-Curtis similarity was used to calculate species differences between groups. The results of the variability analysis were presented on a non-metric

multidimensional scale (NMDS). The differences in gut microbiota composition between groups were analyzed using the PERMANOVA package. Bray-Curtis similarity and NMDS analyses were performed using the phyloseq package [26]. Permutational multivariate analysis of variance (PERMANOVA) was calculated using the microbiome package [27]. The diversity of the gut microbiota was plotted using the MicrobiotaProcess and ggplot2 packages [28]. The phylogenetic trees with the top 150 abundant genera were visualized by GraPhlAn package [29]. The illustration process follow Zhang et al. [30]. The information of core microbiome was identified using phyloseq package (version 1.22.3) [26] with a default prevalence of 0.50 and a detection of 0.0001 for each sample per treatment at genus level. A total of 15 samples were used, combining all three temperature groups (18 °C, 22 °C, and 26 °C). To ensure comparability of read counts across samples, we performed read count normalization. Consequently, given the substantial differences in abundance across genera, we applied a logarithmic transformation to facilitate visualization. The differences between groups were assessed using two-sided t-tests (equal variance) with STAMP (version 2.1.3) [31]. The Bayesian network was constructed using the SAMBA tool [32]. Bacterial taxa were normalized, with zero-count taxa removed, and log-normal distribution applied. Connection strength was assessed using Bayesian Information Criterion (BIC) and Mutual Information (MI), with thresholds set at MI < 0.05 and BIC < 0. PICRUST2 package (version 2.5.1) [33] was used for the prediction of gut microbiota function in KEGG pathway (level 2 and 3) abundance. Statistical analysis of PICRUST2 results was performed by first assessing the normality of data distribution, followed by a Kruskal-Wallis test using STAMP software (version 2.1.3) [31].

Sample Preparing for LC-MS analysis

Four muscle samples from 18°C and 26°C groups were selected for chemical extraction. First, freeze-drying the muscle samples of olive flounder for 24 h by freeze dryer FD4.5-8P-D (KINGMECH, Taiwan) and got ground into fish powder. Then, weigh 400 mg of fish powder and place in a 50 mL plastic sample bottle. Meanwhile, add 10 mL 50% ethanol (Honeywell, USA) and shake in an ultrasonic machine (DELTA ULTRASONIC CO., LTD., Taiwan) for 45 min. Next, filter through ADVANTEC® Qualitative Filter Paper NO.2 (ADVANTEC, Japan) and collect filtrate in 15 mL centrifuge tubes. The filtrate is concentrated by SP Genevac miVac Centrifugal Evaporator (SP Industries, USA) and the residual liquid is removed by freeze dryer. Samples from the previous step were lyophilized and weighed, and the dry weight of the extracted residue was recorded and redissolved at a ratio of 10 mg/mL (dissolved solution: 50% ethanol, Honeywell, USA).

Then, centrifuge 1 mL sample at 14,800 rpm for 3 min in a 1.5 mL centrifuge tube. Finally, 200 μ L of the supernatant was collected for LC-MS analysis.

The condition of chromatography and mass spectrometry

Chromatographic separations were performed on a Q Exactive™ Plus Hybrid Quadrupole-Orbitrap™ Mass Spectrometer (Thermo Fisher Scientific, USA) with an ACQUITY BEH C8 1.7 μ M column (2.1 \times 100 mm) at a column temperature of 40°C. The instrument was operated using Thermo Scientific Xcalibur (version 4.5.445.18) and Freestyle (version 1.8) software. The LC conditions were as follows: mobile phase, (A) 500 mL ddH₂O water + 0.5 mL formic acid; (B) 500 mL acetonitrile + 0.5 mL formic acid; flow rate, 0.4 mL/min; injection volume, positive: 2 μ L, negative: 4 μ L. The gradient elution steps were set as follows: 0 min, 99.5% phase (A) and 0.5% phase (B); 0–6 min, 99.5% phase (A) to 0.5%; 6–8 min, 0.5% (A) and 99.5% (B); 8–8.2 min, 0.5% (A) to 95%; 8.2–10 min, 95% (A) to 99.5%. The properties of Full MS were as follows: resolution, 70,000; AGC target, 1e6; Maximum IT, 60 ms; Scan range, 80 to 1200 m/z.

LC-MS data processing and microbial-metabolite association analysis

The Thermo Xcalibur raw file were converted to mzXML format by ReAdW software (version 4.3.1) (<https://sourceforge.net/projects/sashimi/files/ReAdW> (Xcalibur converter)/), and mzXML data analysis was processed an untargeted metabolites approach by the XCMS online (Version 3.7.1) [34]. Next, the significantly different metabolites were selected as follows criteria: fold change ≥ 1.5 and $p \leq 0.05$. Metabolites annotation was performed using Global Natural Products Social Molecular Networking (GNPS) [35], parameters were set as follows: precursor ion mass tolerance of 0.02 Da, fragment ion mass tolerance of 0.02 Da, minimum pair cosine value of 0.7, minimum matched fragment ions of 6, network TopK of 10, and minimum cluster size of 2. The relative intensity of significant metabolites in significant pathways were selected for heat map analysis via ClustVis [36].

Microbial-metabolite association analysis was performed using the metorigin online platform [37]. The significant metabolites (fold change of ≥ 1.5 and $p \leq 0.05$) which annotated by GNPS were included in the analysis. For bacterial data, only core microbiome with a prevalence of 0.50 were considered. The Mann-Whitney U test (unpaired) was used as the statistical test method, and correlation analysis was performed using the Spearman method.

Results

Quality metrics of nanopore sequencing

To investigate the effect of temperature on bacterial composition, this experiment was conducted using full-length 16 S rRNA gene sequencing with Oxford Nanopore Technologies. The experiment consisted of three temperature groups: low temperature (18°C), medium temperature (22°C) and high temperature group (26°C), each with five biological replicates, resulting in a total of 15 samples. From these samples, a total of 1,754,302 raw reads were generated. Of these reads, 1,752,449 (99.89%) reads were successfully annotated, and 1,746,393 (99.55%) were assigned to the genus level. Detailed statistics are provided in Supplementary File 1, Fig. S1.

The bacterial diversity of gut samples in high- and low-temperature environments

As shown in Fig. 2A, the richness estimates (Chao1) were significantly higher in the 26°C-group compared to the 18°C ($p = 0.0079$, one-way ANOVA) and 22°C ($p = 0.0079$) groups. In contrast, there was no significant difference between the 18°C and 22°C groups ($p = 0.42$). The Shannon index in the 26°C group was the highest among the groups, but it was not significantly different from those in the 18°C and 22°C groups. Variations in Pielou's evenness index also showed no significant differences between the three groups. The similarity of the bacterial community among different groups was assessed using Bray-Curtis dissimilarity with non-metric multidimensional scaling (NMDS). After PERMANOVA analysis, the results revealed a significant effect of temperature on the structure of bacterial community, accounting for 29.9% of the variance ($p = 0.024$). The beta diversity results showed significant differences between the three groups, with the 26°C group being particularly distinct, while the 18°C and 22°C groups were more similar (Fig. 2B). High temperature increases bacterial diversity and shift the structure of gut microbiota.

Taxonomic analysis of the bacterial composition and core Microbiome

The phylogenetic trees were established using GraPhlAn (Fig. 3A). The composition of the gut microbiota from phylum to genus level are shown. The figure presents the 150 genera with the highest abundance, as indicated by the different color segments in the inner circle, which represent the proportional presence of these genera. The outermost heatmap displays the abundance of each species. Genera with an abundance greater than 0.5% are highlighted with a red box (Fig. 3A and Supplementary File 2, Table S1). The results indicate that, in low-temperature environments, the richness proportions of *Alphaproteobacteria* (shown in red), *Betaproteobacteria* (shown in blue), and *Gammaproteobacteria* (shown in purple)

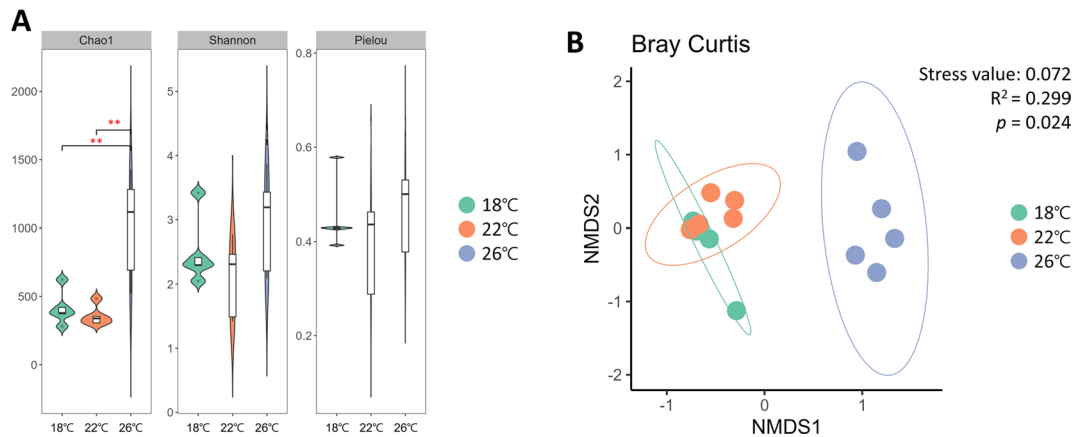


Fig. 2 Diversity analysis of the gut microbiota in olive flounder under varying temperature conditions. **(A)** Alpha diversity metrics: species richness (Chao1 index), diversity (Shannon index), and evenness (Pielou's evenness) across temperature groups (18 °C, 22 °C, and 26 °C; $n=5$). Statistical significance is indicated as $*p \leq 0.05$ and $**p \leq 0.01$; **(B)** Beta diversity analysis using the Bray-Curtis dissimilarity index, showing variation in gut bacterial community composition among the three temperature groups. Non-metric multidimensional scaling (NMDS) was applied, with stress value, R^2 , and p -value provided for the analysis

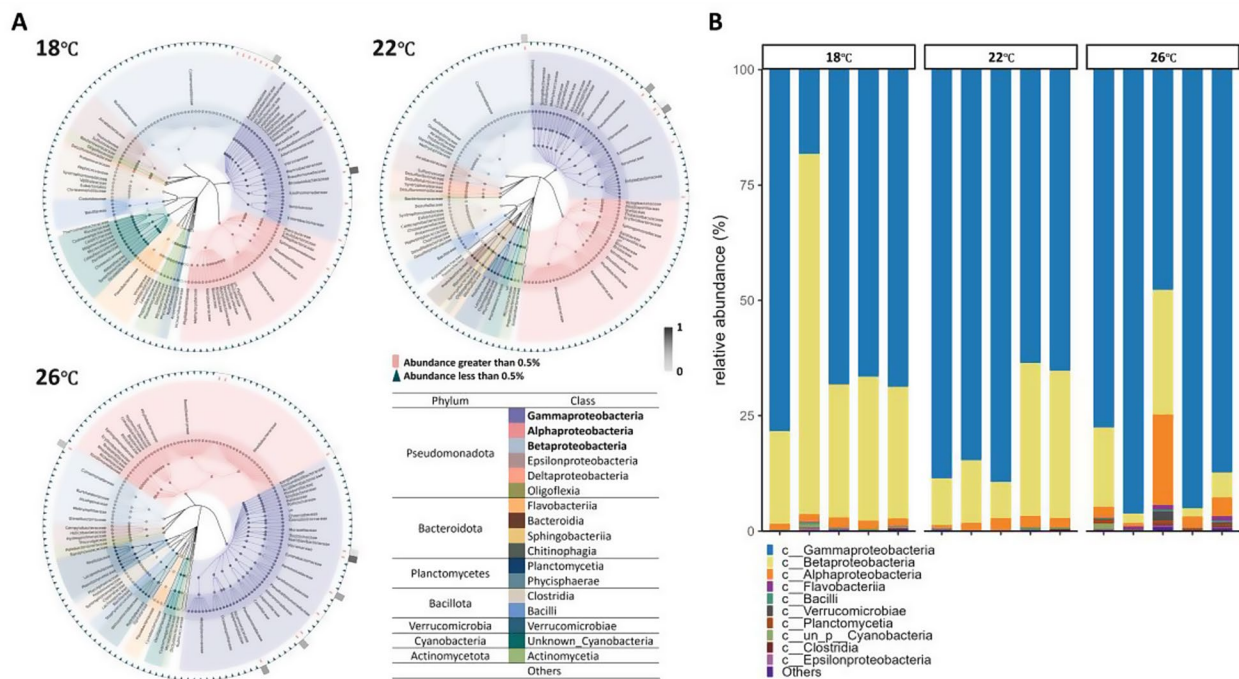


Fig. 3 Bacterial composition and diversity in olive flounder across varying temperature conditions. **(A)** Phylogenetic trees generated by GraPhlAn, illustrating the bacterial composition from the phylum to genus level. Red bars indicate taxa with a bacterial abundance greater than 0.5%, blue triangles represent taxa with an abundance less than 0.5%, and gray bars display a heat map visualization across different samples, the value present the percentage of relative abundance form 0–1. **(B)** Bar chart showing the relative abundance of bacterial classes

are approximately equal, each constituting approximately 21% of the total bacterial population. In contrast, in high-temperature environments, the relative richness of *Alphaproteobacteria* and *Gammaproteobacteria* is significantly higher, whereas the relative richness of *Betaproteobacteria* is lower. At the class level, ten dominant abundance classes were identified in the gut microbiota of olive flounder, including *Gammaproteobacteria*, *Beta*

proteobacteria, *Alphaproteobacteria*, *Flavobacteriia*, *Verrucomicrobiae*, *Bacilli*, *Planctomycetia*, *Cyanophyceae*, *Clostridia*, and *Epsilonproteobacteria*. Among these classes, *Gammaproteobacteria*, *Betaproteobacteria*, and *Alphaproteobacteria* were the three most abundance, regardless of the temperature (Fig. 3B). Comparing temperatures of 18°C to 26°C, *Planctomycetia* was significantly increased at 26°C, while *Betaproteobacteria* significantly degraded

at temperatures higher than 22 °C (Supplementary File 1, Fig. S2).

The concept of the core microbiome, which refers to organisms that are consistently present in a given ecosystem, can be defined in terms of prevalence as the proportion of a given ecological community in which a species or set of species occurs. To understand the core microbiota in gut samples across different temperature treatments, the core microbiome information was collected with a prevalence of 0.50 for each sample per treatment at genus level and with a detection threshold of 0.0001 (Fig. 4A and supplementary file 2, Table S2). We observed a significant shift in the core microbial community structure at higher temperature groups (Fig. 4A). The total number of genera in the core microbiomes was 97, with 6, 3, and 63 genera appearing exclusively in 18°C, 22°C and 26°C groups, respectively, while 16 genera were shared by all three groups (for a complete list, see supplementary file 2, Table S3). To highlight the most potentially significant genera, 20 genera of core microbiome were collected with a detection threshold of 0.002 (Fig. 4B). The results show that *Variovorax*, *Comamonas*, *Diaphorobacter*, *Rhodoferrax*, *Curvibacter*, and *Hydrogenophaga* appeared almost exclusively in 18°C. *Sphingomonas*, *Enterobacter*, *Mesorhizobium*, *Pseudomonas*, *Stenotrophomonas*

, *Acinetobacter*, *Delftia*, and *Phyllobacterium* were found in all groups and decreased as the temperature increased. *Vibrio* and *Photobacterium* were found in roughly equal numbers in both 22°C and 26°C groups, and almost none in 18°C. *Paenirhodobacter* was most common at 26°C, and almost absent at 18°C. *Alteromonas*, *Legionella*, and *Phaeobacter* were found almost exclusively at 26°C (Fig. 4B). The top three most abundant genera in core microbiome were *Pseudomonas*, *Delftia*, and *Vibrio*. In the 18°C group, *Pseudomonas* had the highest abundance, which decreases as temperature increased. Similar to *Pseudomonas*, the relative abundance of *Delftia* also decreased as temperature increased. The abundance of *Vibrio* was highest at 22°C, followed by 26°C and was almost absent at 18°C.

Functional roles of gut microbiota in Olive flounder

This study primarily aims to investigate how temperature changes influence the muscle metabolome composition of flounder, particularly in relation to key metabolic pathways affecting meat quality and flavor. Carbohydrate metabolism contributes to sweetness and umami taste, lipid metabolism influences fatty acid composition—especially polyunsaturated fatty acids (PUFAs)—and amino acid metabolism is closely associated with flavor

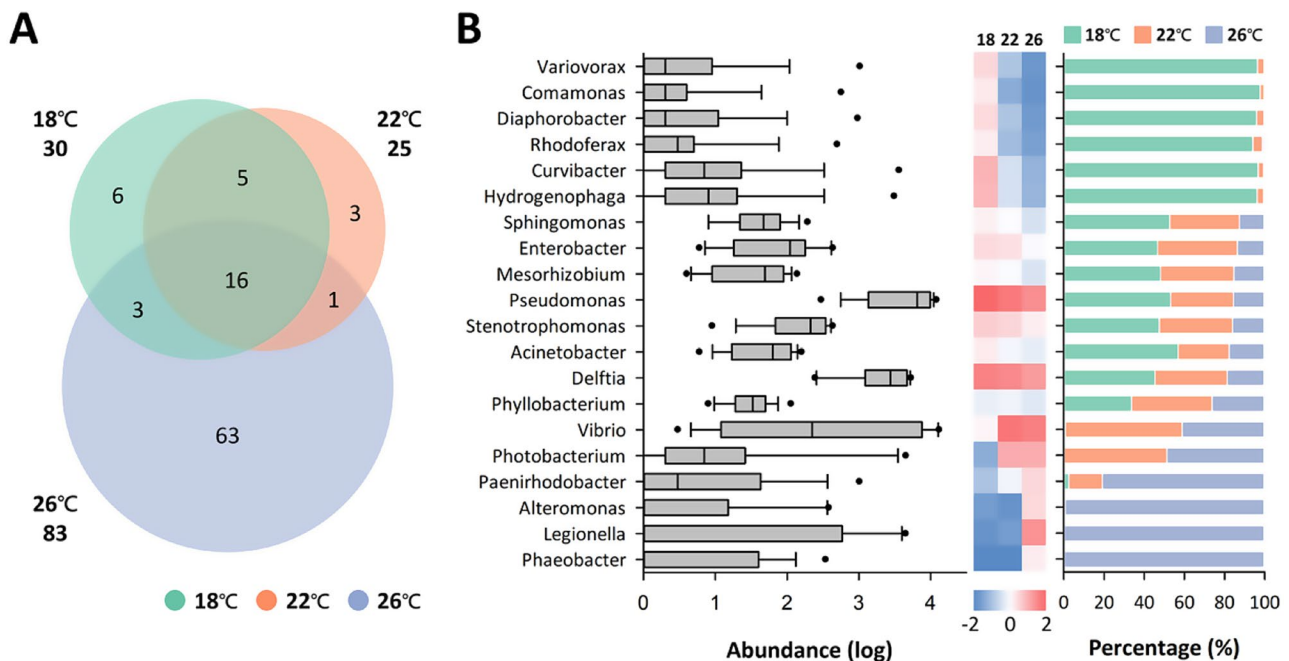


Fig. 4 Core microbiome composition at the genus level in olive flounder across 18°C, 22°C, and 26°C temperature groups. **(A)** Venn diagram illustrating the overlap of core microbiome genera shared among the 18°C, 22°C, and 26°C group, with each core genus having a prevalence of at least 0.50 in the samples per treatment and a detection limit of 0.0001. **(B)** Visualization of the core microbiome's read abundance: The horizontal bar plot displays the log-transformed read count of 20 selected core genera (meeting a prevalence threshold of 0.50 and a detection limit of 0.002) across all samples (n = 15). The heatmap shows the ln(x + 1)-transformed values. Rows are centered; unit variance scaling is applied to rows. The color gradient from red to blue across the map indicates the abundance of core microbiome, with red representing higher relative abundance and blue indicating low. Additionally, the 100% stacked bar plot visualizes the relative contribution of each genus to the total microbial composition, with colored segments representing different genera

compound formation. Given these functional roles, our analysis of microbial functions primarily focused on these metabolic processes. Functional feature prediction was performed using PICRUSt2 based on the Kyoto Encyclopedia of Genes and Genomes (KEGG) database.

In the results of level 2 pathways, the relative abundances of carbohydrate, lipid, and amino acid metabolism decreased in the high-temperature group (22°C and 26°C). However, only carbohydrate and amino acid metabolism in level 2 pathways showed a significant decrease (Fig. 5). In carbohydrate metabolism, the results showed eight level 3 pathways were significantly different ($p \leq 0.05$, Kruskal-Wallis test and Tukey's post-hoc test) (Fig. 5A). The level 3 pathways, including citrate cycle (TCA cycle), glycolysis/gluconeogenesis, glyoxylate, and dicarboxylate metabolism, and propanoate metabolism, had the highest values in the 18°C group. Amino sugar and nucleotide sugar metabolism, pentose phosphate pathway, as well as starch and sucrose metabolism exhibited the lowest levels of activity at 22°C, while showing higher levels of activity at 18°C and 26°C. Galactose metabolic had the highest activity at 26°C, but lower activity at 18°C and 22°C. Similarly, in lipid metabolism, seven KEGG level 3 pathways showed significant differences.

Four pathways at level 3 exhibited the highest levels in the 18°C group, including arachidonic acid metabolism, ether lipid metabolism, fatty acid biosynthesis, and fatty acid degradation ($p \leq 0.05$, Kruskal-Wallis test and Tukey's post-hoc test) (Fig. 5B). Steroid biosynthesis and steroid hormone biosynthesis were highest at 26°C, but lower at 18°C and 22°C. Biosynthesis of unsaturated fatty acids exhibited the lowest levels of activity at 22°C, while showing higher levels of activity at 18°C and 26°C. In amino acid metabolism, seven level 3 pathways, including alanine, aspartate and glutamate metabolism; lysine biosynthesis; phenylalanine metabolism; phenylalanine, tyrosine and tryptophan biosynthesis; tryptophan metabolism; tyrosine metabolism; and valine, leucine and isoleucine degradation, were significantly decreased in both 22°C, and 26°C group. These seven pathways all had the highest values in the 18°C group ($p \leq 0.05$, Kruskal-Wallis test and Tukey's post-hoc test) (Fig. 5C). These results indicate that with increasing temperature, the function of intestinal bacteria in carbohydrate, lipid, and amino acid metabolism was significantly diminished. In addition to the metabolism of carbohydrate, lipid, and amino acid, we also observed that the 18°C group exhibited the lowest levels across all pathways related to energy

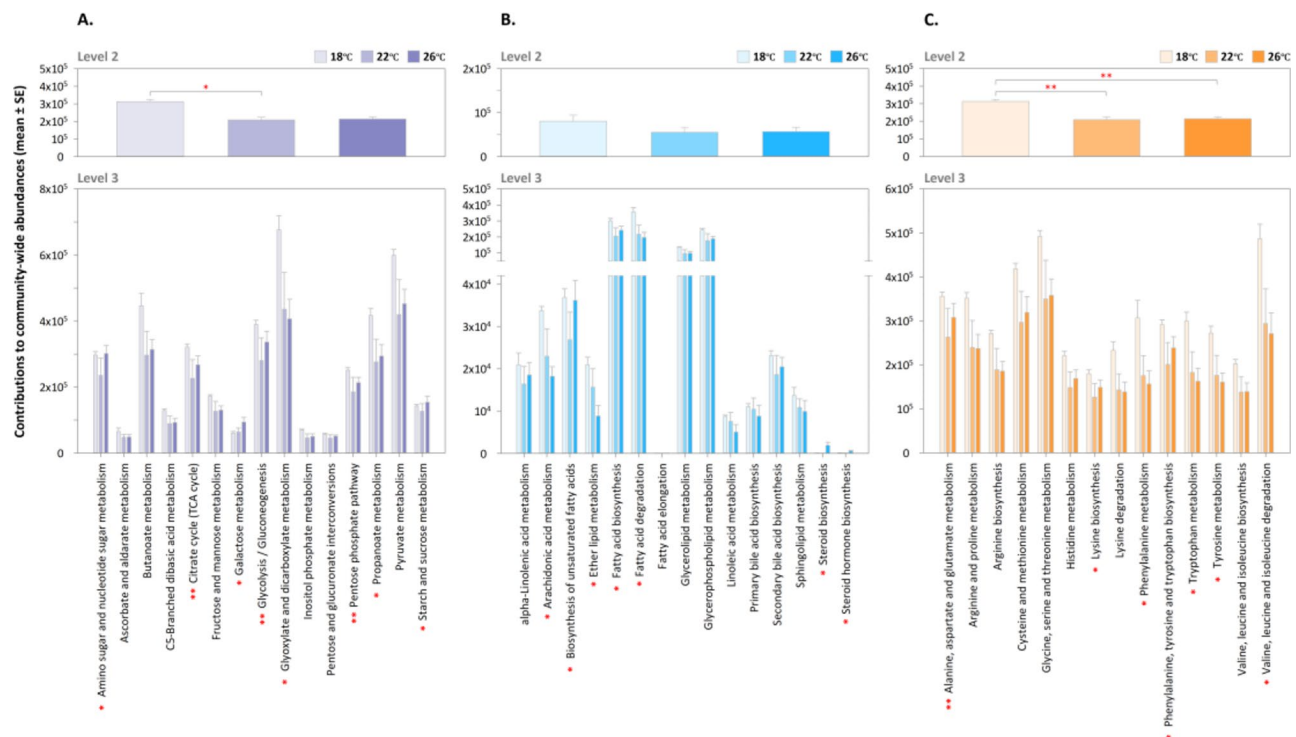


Fig. 5 Predictive functional profiling of microbial communities in olive flounder across different temperature treatments using PICUSt2, focusing on KEGG pathways related to metabolism. The Y-axis represents the contributions to community-wide abundances of KEGG pathways, averaged across samples within each group ($n = 5$). **(A)** Carbohydrate metabolism, **(B)** Lipid metabolism, and **(C)** Amino acid metabolism pathways are depicted. Pathways are categorized into two levels: Level 2 pathways are shown at the top of each panel, represented by a gradient of black to gray colors to indicate varying degrees of pathway abundance. Level 3 pathways, which provide more detailed functional insights, are displayed at the bottom of each panel and are differentiated by purple, blue, and orange colors, respectively. Statistical significance of differences in pathway abundance between groups is indicated by asterisks: * $p \leq 0.05$, ** $p \leq 0.01$

metabolism, including carbon fixation in photosynthetic organisms, carbon fixation pathways in prokaryotes, nitrogen metabolism, oxidative phosphorylation, photosynthesis, and sulfur metabolism. In contrast, the 22°C and 26°C groups showed similarly higher levels in these pathways. Regarding functions associated with stress and oxidative responses, the HIF-1 signaling pathway was lowest in the 18°C group and highest in the 26°C group, whereas glutathione metabolism was lowest in the 26°C group and highest in the 18°C group. All significant functions are provided in Supplementary File 2, Table S4.

Effect of temperature on metabolic compound levels in muscle samples

To determine whether the changes in the gut microbiota under high-temperature conditions can affect muscle tissue, we collected muscle samples from olive flounder cultured at low and high temperatures (18°C and 26°C) and subjected them to untargeted high-resolution LC-MS metabolomic analysis. The principal component analysis (PCA) models show a clear separation between 18°C and 26°C groups (Fig. S3A), demonstrating that the muscle metabolomic profile of flounder can be significantly altered by different culture temperatures. The following criteria were used to identify significantly different metabolites by cloud plot analysis: fold change ≥ 1.5 , $p \leq 0.05$ (Fig. S3B). According to the criteria, 2,593 features are significantly different. In the 26°C group, 1,152 metabolites are upregulated, and 1,441 metabolites are downregulated. All significantly different metabolites are listed in Supplementary file 2, Table S5. Furthermore, amino acids related to flavor were identified, with 14 in the positive group and 5 in the negative group (Supplementary file 2, Table S6 and S7). Nevertheless, only aspartic acid and phenylalanine in the negative group exhibited statistically significant differences. Aspartic acid, which represents umami, exhibited a significantly lower concentration in the high-temperature group ($p = 0.005$). Phenylalanine, which represents the taste of bitterness, was found to be higher in the high-temperature group ($p = 0.02$).

GNPS molecular networking analysis and the structure of significantly different metabolites

To understand the categorization and the associations between significantly different metabolites, GNPS (Global Natural Products Social) molecular network analysis was used to investigate the metabolome of flounder muscle. The results show that 253 metabolites were annotated by the GNPS molecular network analysis, of which 37 exhibited significant differences. Figure 6 displayed the overall GNPS molecular network, where the metabolites annotated by GNPS are shown in pink and the significantly different metabolites are represented in blue. In this

analysis, the primary modules, denoted as A, B, C, and D, are identified based on the preponderance of annotated metabolites within each. Module A is delineated by a composition of 90 metabolites, where 22 are annotated, and 5 are identified as significantly divergent, including metabolites such as arachidonic acid (ARA, m/z 305.247) and eicosapentaenoic acid (EPA, m/z 303.231), among others. Within Module B, a total of 45 metabolites were identified, with 10 bearing annotations and 3 marked by significant differences, including compounds such as arachidonoylcarnitine (m/z 448.341), L-Acetylcarnitine (m/z 204.123), and L-Hexanoylcarnitine (m/z 260.185). Module C, however, details 30 metabolites, with a substantial 23 annotated and 3 showing significant differences, notably PC(18:3/18:3) (m/z 778.536), PC(14:0/16:1) (m/z 704.521), and arachidonoylthio-PC (m/z 784.583). Module D contains 24 metabolites, of which 18 are annotated and 2 are significantly altered, namely lysoPC(P-16:0) (m/z 480.343) and lysoPC(P-18:0) (m/z 508.375). Figure 7 presents a heatmap illustrating the relative intensities of the 37 significantly altered metabolites, providing a visual representation of metabolite intensity distribution across various samples. Each heatmap cell is dedicated to a unique metabolite and sample pairing, with color intensity reflecting the metabolite's relative abundance in that sample.

The correlation analysis of metabolic compounds and microbiota in Olive flounder

From the results concerning the functional roles of gut microbiota (referenced Fig. 5B), it was found that level 3 lipid biosynthesis-related pathways were significantly downregulated in the high temperature group. Coincidentally, the data presented in Fig. 7 also suggest that several lipid-related metabolites were significantly downregulated in the high temperature group. To investigate the relationship between gut microbiota and muscle metabolism, the sources of 37 metabolites were analyzed utilizing the MetOrigin tool. MetOrigin is highly adept at rapidly identifying metabolites associated with microbiota and elucidating their functions in metabolomics research. The Sankey network visualization, a graphical representation of statistical and biological associations, effectively demonstrates the connections between particular microbes and the metabolites. Figure 8A and B shows the identified metabolites, which include 2 host metabolites, 1 microbial metabolite, 14 host and microbial co-metabolites and 20 other metabolites, comprising 1 drug-related, 10 food-related and 9 unknown metabolites. Metabolic pathway analysis showed 14 KEGG pathways annotated for the host, microbiome, and co-metabolic activities (host and microbiome), as illustrated in Fig. 8C. Among these pathways, the majority (12 out of 14) were based on co-metabolism, while 2

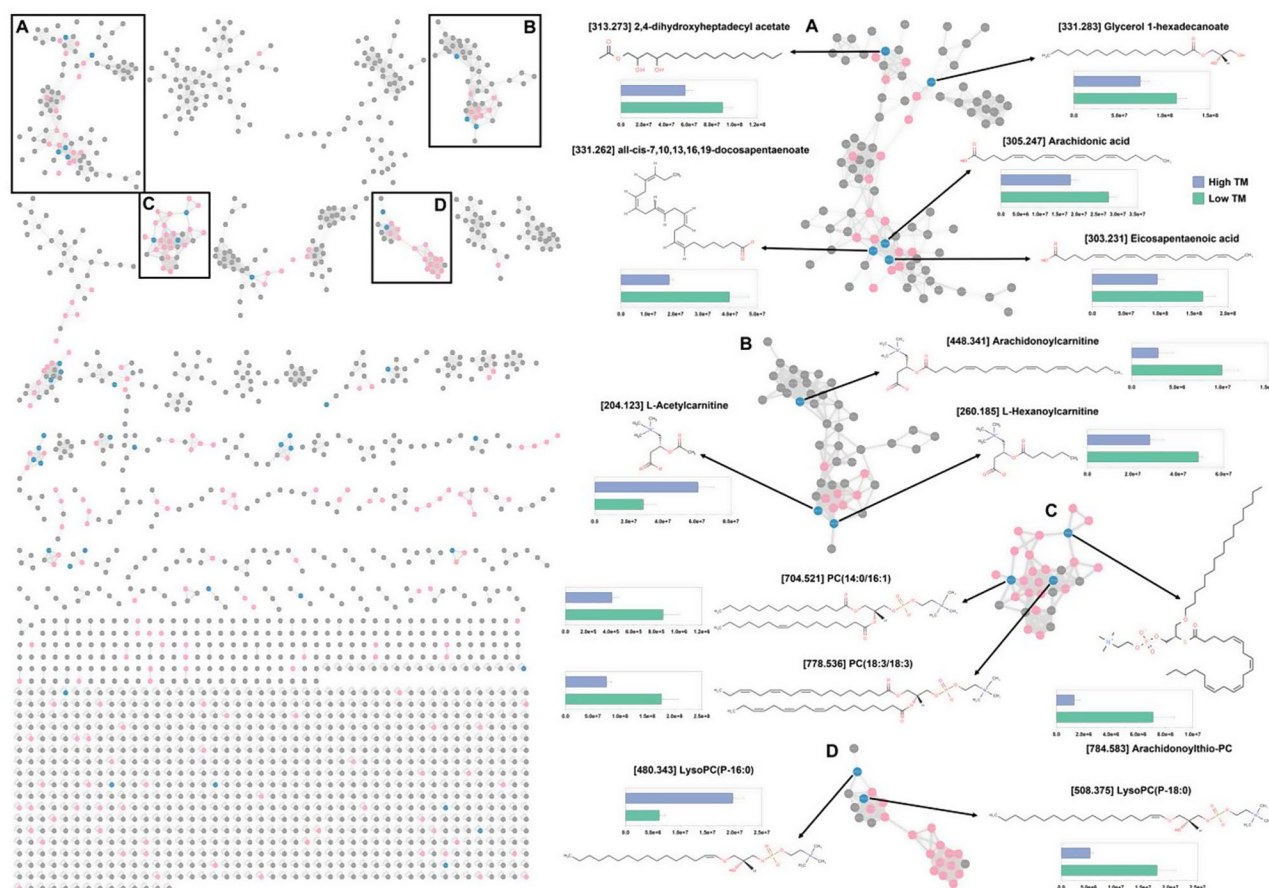


Fig. 6 Molecular networking and differential metabolite analysis in olive flounder across low and high temperature treatments. Molecular networking is visualized, where annotated metabolites are highlighted in pink, indicating their identification based on known databases. Metabolites with significant differences between temperature groups are marked in blue. The thickness of the connecting lines represents the cosine similarity score, indicating the structural similarity between metabolites. Accompanying the molecular network, a bar graph compares the intensity values of metabolites, representing their relative abundance or concentration. The low temperature group is depicted in blue, while the high temperature group is shown in green

were attributed to the host and 1 to the microbiome. The pathways showing significant differences included those involved in glycerophospholipid metabolism, arachidonic acid metabolism, the biosynthesis of unsaturated fatty acids, caprolactam degradation, glycosylphosphatidylinositol (GPI)-anchor biosynthesis, linoleic acid metabolism, alpha-linolenic acid metabolism, and streptomycin biosynthesis.

The Sankey network visualization further elucidated the pronounced distinctions among the pathways and their interconnections with the microbiota. As depicted in **Fig. S4**, genera such as *Comamonas*, *Delftia*, *Enterobacter*, and *Stenotrophomonas* emerged as key contributors in the catabolism of glycerophospholipids, linoleic acid, and alpha-linolenic acid. These bacteria significantly positively affected the metabolites phosphatidylcholine (PC, KEGG compound ID: C00175). On the other hands, *Marinicella*, *Photobacterium* and *Tritonibactor* were found to have a significant negative correlation with these metabolites. Notably, there was a significant decrease in

the relative abundance of *Comamonas* and *Stenotrophomonas* in the gut microbiota, while *Marinicella* and *Tritonibactor* exhibited a significant increase.

In the biosynthetic pathway of unsaturated fatty acids, it was observed that the concentrations of two major metabolites were lower in a high-temperature environment: arachidonic acid (ARA) (Fig. S5) and eicosapentaenoic acid (EPA) (Fig. S6). Sankey network analysis revealed considerable similarity among the microbiota involved in ARA and EPA metabolism, with 13 primary classes demonstrating a significant negative correlation. Interestingly, the levels of *Alphaproteobacteria*, *Planctomycetia*, *Flavobacteria*, *Verrucomicrobiae*, and *Actinomyetia* in the gut microbiota exhibited a significant upward trend. However, notable differences were observed in the correlation between *Pseudomonas* and the metabolites ARA and EPA. The genus *Pseudomonas*, however, only demonstrated a significant positive correlation with the biosynthesis of EPA (Fig. S6).

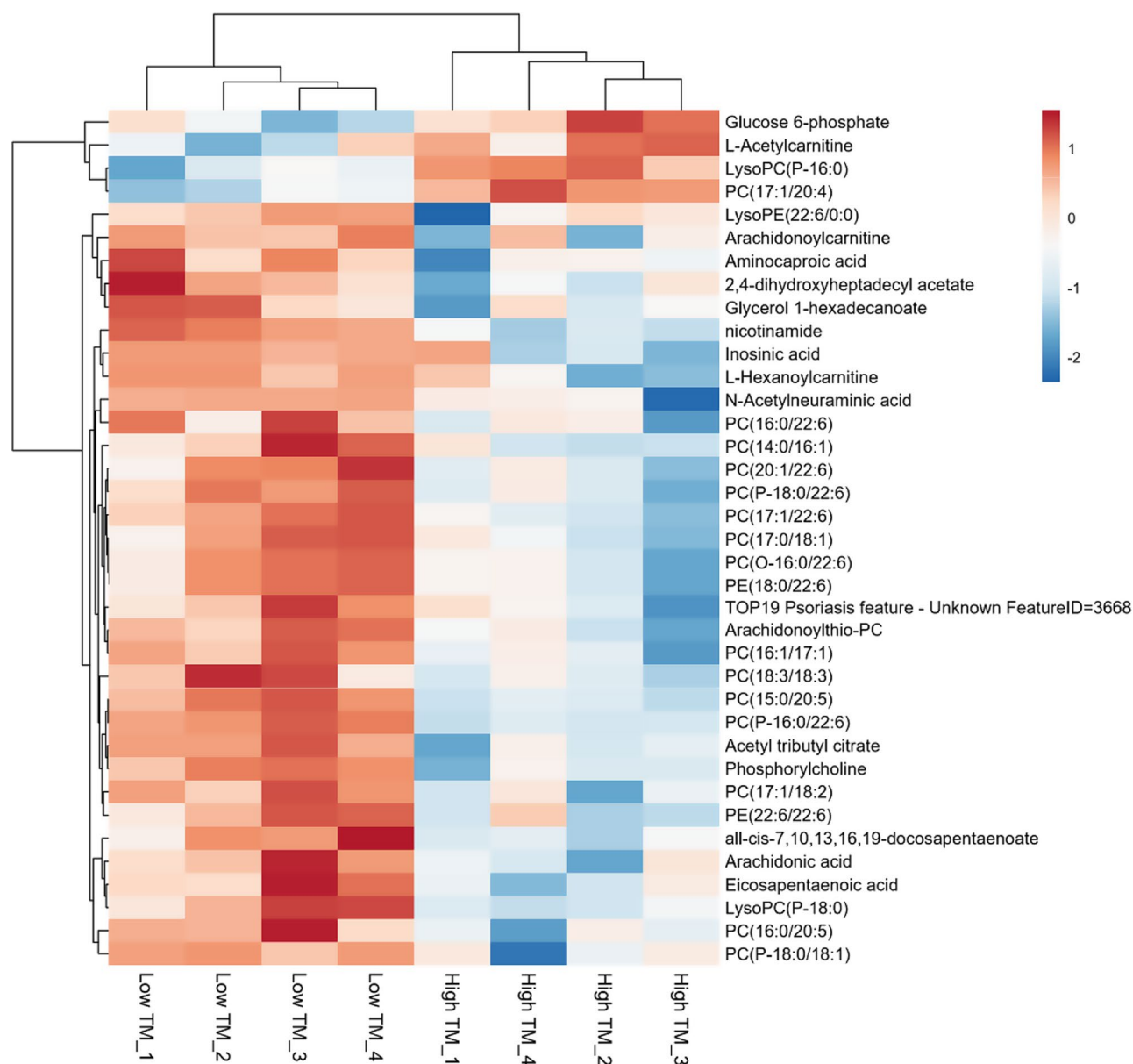


Fig. 7 Differential metabolite profiles in the muscle tissue of olive flounder across low and high temperature treatments. This heatmap analysis illustrates the relative intensity of metabolites that show significant differences in abundance. Each row corresponds to a specific metabolite, with the names labeled on the right. Original values are $\ln(x+1)$ -transformed. Rows are centered; unit variance scaling is applied to rows. Both rows and columns are clustered using correlation distance and average linkage. The color gradient from red to blue across the map indicates the level of metabolite intensity, with red representing high intensity (or higher relative abundance) and blue indicating low intensity (or lower relative abundance)

Figure 9 presents a summary of the microbial-metabolite association network, illustrating the relationship between 12 significantly different metabolites and six key bacterial genera. It could be observed that the abundances of *Legionella* and *Phaeobacter* were significantly higher in the high-temperature group (indicated by red borders) and were significantly positively correlated with LysoPC(P-16:0) and glucose 6-phosphate (indicated by red solid lines). Conversely, both genera were negatively correlated with LysoPC(P-18:0), PC (14:0/16:1), PC (16:0/25:0), PC(15:0/20:5), PC(18:3/18:3), EPA, and ARA

(indicated by blue solid lines). In contrast, the genera *Pseudomonas*, *Stenotrophomonas*, *Sphingomonas*, and *Comamonas* were presented in significantly lower amounts in the high-temperature group (indicated by blue borders) and were mainly positively correlated with metabolites related to phosphorylcholine and PCs (red solid lines).

Discussion

Climate change and rising water temperatures are major concerns for aquaculture, especially for cold-water species like flounder. The impact of elevated temperatures

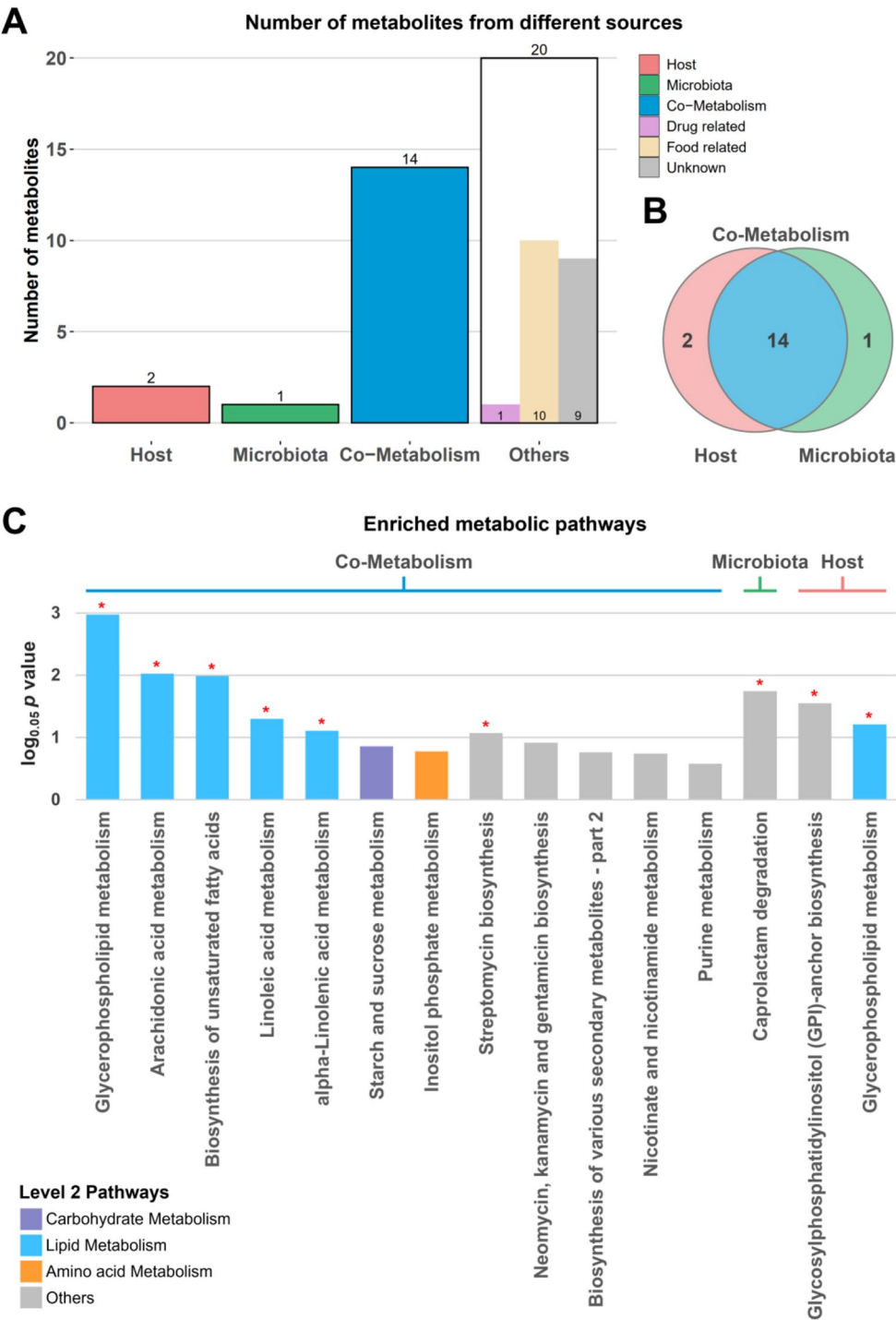


Fig. 8 MetOrigin analysis on the gut microbiota and muscle metabolites between the low and high temperature groups. **(A)** Bar plot and **(B)** Venn diagram of the number of significantly different metabolites in different sources. **(C)** Metabolic pathway enrichment analysis (MPEA) of these significantly different metabolites in different categories. Bar colors indicate different KEGG L2 pathways. Significant differences ($p \leq 0.05$) are marked with a red asterisk (*). At the top of the figure, text and horizontal lines indicated sources classification of enriched metabolic pathways

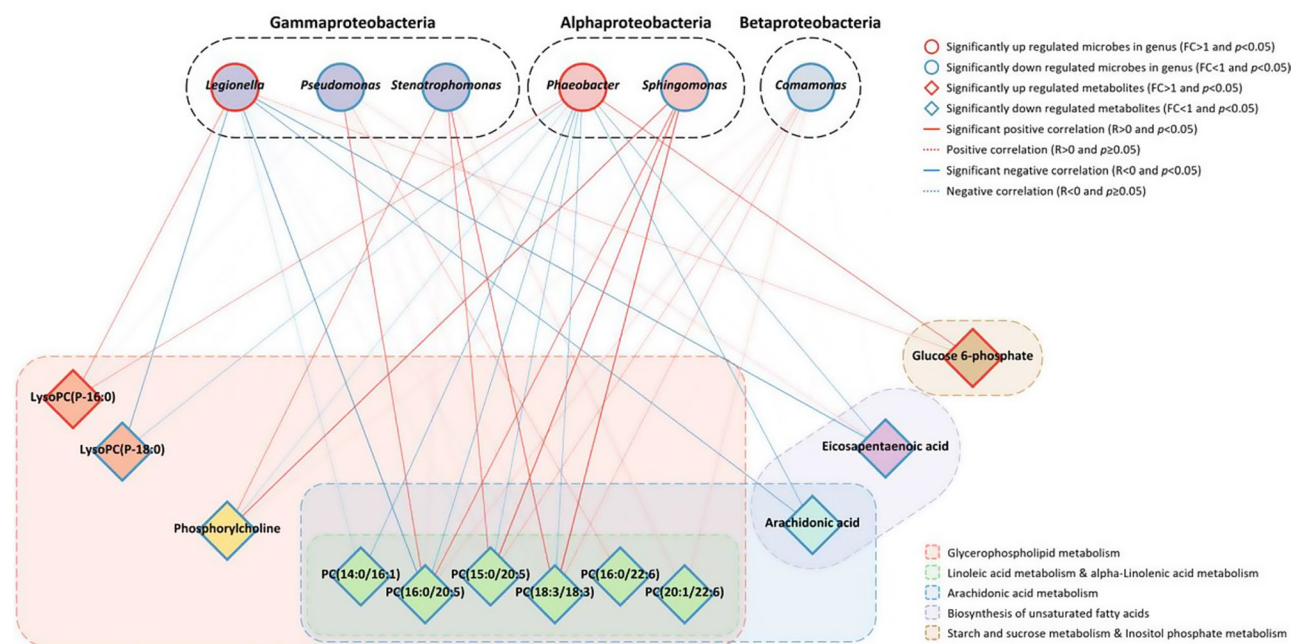


Fig. 9 The network summary of microbial-metabolite association. Colored squares represent metabolic pathways. Diamonds and circles depict metabolites and microbes, respectively, that have shown significant differences in abundance. Nodes frames are colored red and blue to indicate up-regulation and down-regulation, respectively. Connections between nodes are illustrated with lines, where red and blue lines represent positive and negative correlations, respectively. Darker shades of red and blue lines denote correlations that are significantly strong

on fish health is becoming more evident, as it influences not only growth rates and reproduction but also the gut microbiota, which plays a key role in host nutrition, immunity, and resilience to environmental stressors [38]. As poikilothermic organisms, fish are directly affected by temperature fluctuations, which can induce significant changes in their internal metabolic processes, including those linked to the gut microbiota and muscle metabolism.

Recent studies have shown that water temperature can affect gut microbiota in various fish species. For example, a study on greater amberjack demonstrated that increasing water temperatures (from 24°C to 33°C) led to shifts in gut microbiota composition, which were associated with reduced fish growth [39]. Similarly, in rainbow trout, heat stress at a temperature of 24°C (higher than their optimal 16°C) caused imbalances in gut microbiota, which affected lipid and amino acid metabolism—two critical pathways for fish health [40]. Considering these findings, it is crucial to understand how temperature-induced shifts in gut microbiota and metabolism may affect the overall health and growth of aquaculture species.

In this study, we focused on investigating how different temperature conditions (18°C, 22°C, and 26°C) affect the gut microbiota and muscle metabolome of olive flounder (*P. olivaceus*). We found that higher temperatures significantly altered the composition of the gut microbiota, with increased diversity observed at elevated

temperatures (Fig. 2). This result is consistent with previous findings by Neuman et al. [41], who observed that Atlantic salmon collected during warmer months showed a higher diversity of gut microbiota compared to those collected during colder months. This demonstrates that increased temperatures lead to gut microbiota alterations in flounder, similar to other fish species, potentially affecting their health and metabolic processes.

The vertebrate gut microbiota is typically dominated by the phyla *Bacillota*, *Bacteroidota*, *Actinomycetota*, *Pseudomonadota*, and *Fusobacteria*. In mammals, the phyla *Bacillota* and *Bacteroidota* are the dominant members of the gut microbiota. In contrast, in many birds, reptiles, and fish, the phylum *Pseudomonadota* represents a larger proportion of the gut microbial community [42]. Regarding the gut microbiota in animals, while each host species exhibits distinct microbial responses to heat stress, certain bacterial groups in the gut demonstrate consistent alterations in response to temperature fluctuations across different hosts [43].

In mammals, it has been demonstrated that temperature has a negative effect on the relative abundance of the gut bacterial phylum *Bacillota*, such as cattle [44] and mice [45]. In fish (rainbow trout), a negative correlation between rearing temperature and the relative abundance of *Bacillota* has been observed [46]. This study (Fig. 3) indicates that the group of *Pseudomonadota* exhibited the greatest richness and abundance among the olive flounder examined across a range of water temperatures.

This finding was consistent with previous studies, which demonstrated that the relative abundance of *Pseudomonadota* was higher in fish species [42]. Additionally, it aligned with previous research on flounder, in both wild and farmed olive flounder, as well as across various growth stages [47] and under different aquafeed [38, 47]. The top three dominant classes were *Alphaproteobacteria*, *Betaproteobacteria*, and *Gammaproteobacteria*, all belonging to the phylum *Pseudomonadota*. There was an increase in *Alphaproteobacteria* and *Gammaproteobacteria* and a decrease in *Betaproteobacteria* in the group at 26 °C. *Gammaproteobacteria*, the largest class within *Pseudomonadota*, includes common potential pathogenic bacteria such as *Enterobacteriaceae*, *Vibrionaceae* and *Seudomonadaceae* [48]. A recent study on the gut microbiota of Atlantic salmon (*Salmo salar*) [41] and yellow-tail kingfish (*Seriola lalandi*) [49] found that increased temperature is associated with changes in the relative abundance of *Gammaproteobacteria*. The present study also observed similar changes in the abundance of *Gammaproteobacteria* (Fig. 3). It can be reasonably concluded that the observed alterations in the composition of the gut microbiota in flounder as a consequence of temperature fluctuations are largely attributable to fluctuations in the relative abundance of the *Pseudomonadota*. Furthermore, keeping flounder continuously at 26 °C may increase the risk of pathogen infection. These findings indicate that temperature regulation may be a more effective strategy for preserving a balanced gut microbiota in cultured flounder.

Some dominant genera were identified within the gut microbiota of olive flounder (Fig. 4), with *Pseudomonas*, *Delftia*, and *Vibrio* being the top three. *Pseudomonas*, a diverse genus known for its wide metabolic capabilities, broad ecological distribution, and adaptability to various environments, has strains that have been utilized as probiotics in the aquaculture industry [50]. Our findings highlight that *Pseudomonas* was the most prevalent genus, especially within the 18 °C group, potentially enhancing the metabolic efficiency of flounder in colder environments [51]. Furthermore, Niu et al. [47] observed that *Delftia* predominated in both juvenile and subadult stages, corroborating our findings that *Delftia* was prevalent across all experimental groups. Several species within the *Vibrio* and *Photobacterium* genera have been identified as opportunistic pathogens in flounder. These microorganisms, which are prevalent in marine ecosystems, can induce disease in fish [52]. Shao et al. have demonstrated that some species of *Sphingomonas* and *Acinetobacter* exhibit significantly higher capacities for the assimilation of ammonia nitrogen, nitrite nitrogen, and total phosphorus [53]. As illustrated in Fig. 4, the abundances of *Vibrio* and *Photobacterium* exhibited a notable increase at temperatures of 22 °C and

26 °C. Conversely, the abundances of *Sphingomonas* and *Acinetobacter* exhibited a gradual decline as the temperature increased. This suggests that elevated temperatures may have a detrimental impact on the health of flounder, potentially increasing the risk of disease and reducing the capacity for ammonia nitrogen decomposition [54]. The presence of *Phaeobacter* was observed in the 26 °C group. Previous research has indicated that *Phaeobacter* has been utilized as a probiotic, demonstrating efficacy in inhibiting the growth of *Vibrio* species and against *Vibrio* infections [55]. This observation may explain the lower abundance of *Vibrio* at 26 °C compared to the 22 °C group.

To elucidate the functions associated with variations in the microbial community, we employed the Phylogenetic Investigation of Communities by Reconstruction of Unobserved States (PICRUSt2) to predict the gut microbiota's functional profile. The results revealed that Kyoto Encyclopedia of Genes and Genomes (KEGG) Level 2 pathways, including those related to carbohydrate, lipid, and amino acid metabolism, were significantly more active in the group maintained at a lower temperature (18 °C) compared to those at higher temperatures (22 °C and 26 °C), as illustrated in Fig. 5. Hu et al. [56] reported findings consistent with ours, observing that enzymes involved in glycolysis/gluconeogenesis, lipid metabolism, and protein digestion and absorption were enriched in the transcriptomic analyses following exposure to low temperatures. They proposed that increased energy metabolism activities are mobilized to mitigate the effects of a cold environment. Similar conclusions were drawn in previous research, which highlighted that amino acid metabolism plays a crucial role in regulating the body's energy and protein balance, thereby supporting the growth and survival of gut bacteria [57, 58]. Our findings demonstrate that different temperature environments significantly influence gut microbiota function, especially in energy regulation and metabolism. In flounder, enhanced energy metabolism activities were observed at lower temperatures.

In addition to gut microbiota, temperature also affects muscle metabolites. In this study, muscle metabolomics analysis highlighted a notable reduction in polyunsaturated fatty acids (PUFAs), specifically eicosapentaenoic acid (EPA) and arachidonic acid (ARA), in the high temperature group (Figs. 6 and 7). Concurrently, a decrease was also observed in phosphatidylcholine (PC) species containing PUFAs, including PC (15:0/20:5), PC (18:3/18:3), PC (16:0/20:5), PC (16:0/22:6), and PC (20:1/22:6). Research indicates that phosphatidylcholine, a crucial phospholipid for eukaryotic membrane formation, can be synthesized through either the CDP-choline pathway or the methylation pathway [59]. Moreover, phosphatidylcholine is known to undergo fatty acid

remodeling within the membrane, thereby ensuring the maintenance of its metabolic functions [60]. Consequently, these findings may be attributed to the necessity for a greater proportion of PUFA-rich PC in low-temperature environments to enhance cell membrane fluidity. Moreover, the literature indicates that fish species that inhabit cold-water environments typically exhibit higher levels of PUFA compared to those that inhabit temperate environments [61].

A deficiency in PUFAs may have a detrimental impact on the survival, growth, and development of flounder [62, 63]. Moreover, these fatty acids facilitate proper pigmentation [64], enhance reproductive outcomes [65], and promote superior egg quality [65]. Given the importance of flounder as an aquatic product and a source of protein for humans, it is of crucial importance to understand the PUFA content of flounder. Nevertheless, as with all vertebrates, fish are unable to biosynthesize PUFAs *de novo* from saturated and monounsaturated fatty acids [66]. Marine fish primarily obtain their long-chain PUFAs (LC-PUFAs) from the producers of PUFAs in the marine ecosystem [67], including photosynthetic microalgae, heterotrophic protists, and bacteria [68]. Additionally, it is well-documented that bacteria capable of producing long-chain PUFAs (LC-PUFAs), such as ARA, EPA, and DHA, predominantly reside in the intestines of fish in cold-water environments [69]. This indicates that flounder in cold water environments produce more PUFAs, which is influenced by gut microbiota. Our findings appear to corroborate this, as both the functional predictions of gut microbiota (Fig. 5) and the metabolomic results from muscle tissue (Fig. 7) indicate an increase in the synthesis of PUFAs and related metabolites in low-temperature environments. In addition to PUFA, the flavor of fish meat may be directly impacted by temperature. Research indicates that aspartic acid is an important source of umami [70], whereas phenylalanine is associated with bitterness [71]. The results of this study indicate that the muscle metabolite aspartic acid significantly decreases, while phenylalanine significantly increases at high-temperature conditions in flounder. This indicates that the umami flavor of flounder is diminished and bitterness is enhanced under high-temperature conditions (Supplementary file 2 Table S5). Previous research has demonstrated that *Pseudomonas* is involved in the metabolism of aspartic acid and phenylalanine, thereby supporting this hypothesis [72, 73].

To elucidate the relationship between gut microbiota and their influence on flounder metabolism, MetOrigin analysis was employed in this study. The findings revealed that out of 37 metabolites analyzed, 14 metabolites were implicated in co-metabolism (Fig. 8A and B), indicating a potential involvement of the microbiota in muscular metabolic processes. Notably, these metabolites were

primarily associated with lipid metabolism (Fig. 8C). Similarly, functional feature prediction of microbial communities revealed comparable findings, whereby the pathway of arachidonic acid metabolism and the biosynthesis of unsaturated fatty acids exhibited significant differences in both gut microbiota (Fig. 5B) and muscle metabolites (Fig. 8C). This evidence suggests that the gut microbiota plays a pivotal role in regulating lipid metabolic pathways in flounder.

In the correlation analysis, two bacterial genera were identified, including *Legionella* and *Phaeobacter*, which exhibited similar patterns and were found to be significantly positively correlated with LysoPC(P-16:0) and G6P. In contrast, they exhibited a significantly negative correlation with LysoPC(P-18:0), PC(14:0/16:1), PC(16:0/20:5), PC(15:0/20:5), PC(18:3/18:3), ARA, and EPA. (Fig. 9). Research indicates that some bacteria possess high phospholipase activity, which enables them to effectively decompose PC into LysoPC and free fatty acids, such as *Legionella* [74]. In our study, we also observed the upregulation of LysoPC (P-16:0) and the downregulation of PC (16:0/20:5), which suggests that *Legionella* and *Phaeobacter* may have high phospholipase activity, effectively decomposing PC (16:0/20:5) into LysoPC (P-16:0) and free fatty acids. Moreover, studies had indicated that *Phaeobacter* plays a significant role in carbon and sulfur metabolism. It is involved in central carbon metabolism by phosphorylating glucose to produce G6P [75]. Our results also supported this observation (Fig. 9), where *Phaeobacter* and G6P levels were higher in high-temperature environments compared to low-temperature environments, with a significant correlation difference. Furthermore, it was observed that *Comamonas*, *Pseudomonas*, *Sphingomonas*, and *Stenotrophomonas* exhibited a significant positive correlation with PC(16:0/20:5), PC(15:0/20:5), and PC(18:3/18:3). Notably, *Pseudomonas* was the sole genus to demonstrate a significant positive correlation with EPA. This observation is consistent with existing literature, which indicates that *Pseudomonas* is the only genus among those mentioned that is known for its capacity to produce PUFAs [76]. Despite the absence of direct evidence in the literature linking *Stenotrophomonas* and *Sphingomonas* with the synthesis of PUFAs, studies have indicated that *Stenotrophomonas* is an efficient bacterium for the hydration of unsaturated fatty acids. Meanwhile, *Sphingomonas* interacts with a species of microalgae (*Oocystis* sp.), which enables *Oocystis* sp. to produce higher amounts of linolenic acid and EPA [77]. This indicates that *Sphingomonas* may also influence the efficacy of other PUFA producers in flounder. Consequently, the observed decline in PC-related metabolites in high-temperature environments can be attributed to the reduction in fatty acid synthesis resulting from the diminished presence of these bacteria.

The results of functional prediction and the enriched metabolic pathways indicated a direct link between gut bacteria and host metabolism. The gut microbiota is capable of regulating the host's carbohydrate, amino acid, and lipid metabolism, with a particular impact on lipid metabolism. This regulation not only affects the abundance of PUFA and PC-related metabolites but also the flavor of the fish. Some bacterial genera exhibited significant correlations with these metabolites, namely *Pseudomonas*, *Sphingomonas*, and *Stenotrophomonas* (positive correlation), along with *Legionella* and *Phaeobacter* (negative correlation). Furthermore, we evaluated microbial interactions under different temperature conditions using a probabilistic analysis with the SAMBA tool [32]. The results suggest a potential causal relationship between temperature and bacterial taxa associated with PUFA- and PC-related compounds linked to host lipid metabolism. Several genera associated with these compounds exhibited either direct (*Pseudomonas* and *Legionella*) or indirect (*Phaeobacter* and *Sphingomonas*) interactions with temperature, while *Stenotrophomonas* was positioned at the final node in the network (Fig. S7). These findings support a significant causal relationship between temperature and these bacterial taxa.

The Bayesian network highlights the central role of temperature in shaping microbial interactions, with multiple genera either directly or indirectly influenced by temperature variation. This observation aligns with previous studies identifying temperature as a key environmental driver of microbiome composition. The identification of microbial taxa associated with PUFA (polyunsaturated fatty acids) and PC (phosphatidylcholine)-related compounds suggests that these microbes may contribute to host lipid metabolism or dietary fat utilization. These findings may have broader implications for understanding microbiome-mediated metabolic processes under variable environmental conditions, such as those driven by climate change.

These genera have the potential to serve as biomarkers in cold-water fish. Notably, the positively significant correlation genera are promising candidates for development into probiotics for aquaculture. In summary, this study introduces a novel perspective on the symbiotic relationship between the host and its microbiome in adapting to environmental changes.

Conclusions

In conclusion, this comprehensive study elucidates the interaction between environmental temperature, gut microbiota, and metabolite composition in flounder. Our analysis of gut bacteria revealed that elevated temperatures significantly enhance the diversity and alter the composition of the gut microbiota, which in turn impacts the carbohydrate, lipid, and amino acid metabolism in

flounder. Moreover, the gut microbiota also affects the metabolism and flavor of the host's muscles. Notably, muscle metabolite analysis revealed a significant decrease in PUFAs and PC-related metabolites in the high-temperature groups. The results indicated that *Comamonas*, *Pseudomonas*, *Sphingomonas*, and *Stenotrophomonas* were positively correlated with the levels of PUFAs and PC-related metabolites. This suggests that these bacteria may have great potential for future applications. In recent years, the temperature increases caused by climate change have emerged as a significant source of stress for aquatic organisms. This study represents the first attempt to describe the effects of low and high temperature environments on the gut microbiome and muscle metabolome of the olive flounder (*Paralichthys olivaceus*). It is anticipated that the findings will address the issues caused by climate change, reduce disease and mortality rates, and enhance the quantity and quality of aquaculture production.

Availability of supporting data

The raw data of gut microbiota has been deposited to the NCBI (BioProject: PRJNA993814) and raw metabolomics data has been deposited to the Mass spectrometry interactive virtual environment (MassIVE Accession: MSV000094177).

Abbreviations

ANOVA	Analysis of variance
ARA	Arachidonic acid
CDP-choline	Cytidinediphosphocholine
DHA	Docosahexaenoic acid
EMBL-EBI	European Molecular Biology Laboratory's-European Bioinformatics Institute
EPA	Eicosapentaenoic acid
FAO	Food and Agriculture Organization
GNPS	Global natural products social
HR-MS	High-resolution mass spectrometry
KEGG	Kyoto Encyclopedia of Genes and Genomes
LC	Liquid chromatography
LC-PUFAs	Long-chain polyunsaturated fatty acids
NCBI	National Center for Biotechnology Information
NMDS	Non-metric Multidimensional Scaling
ONT	Oxford Nanopore Technology
<i>P. olivaceus</i>	<i>Paralichthys olivaceus</i>
PBS	Phosphate buffered saline
PC	Phosphatidylcholine
PCA	Principal component analysis
PCR	Polymerase chain reaction
PERMANOVA	Permutational multivariate analysis of variance
PICRUST2	Phylogenetic Investigation of Communities by Reconstruction of Unobserved States 2
PKS	Polyketide synthase
PUFAs	Polyunsaturated fatty acids
rRNA	Ribosomal ribonucleic acid
STAMP	Statistical Analysis of Metagenomic Profiles
XCMS	EXtensible Computational Mass Spectrometry

Supplementary Information

The online version contains supplementary material available at <https://doi.org/10.1186/s42523-025-00417-9>.

Supplementary Material 1

Supplementary Material 2

Acknowledgements

We thank the Mass Spectrometry Core Facility, Biomedical Translation Research Center (BioTRC), Academia Sinica, Taiwan for sample analysis and technical advice on flounder muscle.

Author contributions

C.C.C: Formal analysis, Investigation, Data Curation, Visualization, Writing - Original Draft. Y.P.C: Methodology, Validation, Investigation, Data Curation, Resources. H.T.Y: Methodology, Validation, Investigation, Data Curation. Y.L.C: Methodology, Validation, Investigation, Data Curation. C.W.W: Methodology, Validation, Investigation, Data Curation. H.Y.G: Conceptualization, Supervision. Y.S.H: Conceptualization, Data Curation, Resources, Supervision, Project administration, Funding acquisition. Y.N.O: Conceptualization, Data Curation, Visualization, Writing - Review & Editing, Resources, Supervision, Project administration, Funding acquisition.

Funding

This research was financially supported by grants (110AS-1.3.2-ST-aT, and 112AS-1.3.2-ST-aG) from the Ministry of Agriculture, Taiwan to Yuan-Shing Ho and Ying-Ning Ho.

Data availability

The raw data of gut microbiota has been deposited to the NCBI (BioProject: PRJNA993814) and raw metabolomics data has been deposited to the Mass spectrometry interactive virtual environment (MassIVE Accession: MSV000094177).

Declarations

Ethics approval

This animal study adhered to the ethical guidelines and protocols approved by the Institutional Animal Care and Use Committee (IACUC) of National Taiwan Ocean University. All experimental procedures were conducted in strict accordance with the ARRIVE (Animal Research: Reporting of In Vivo Experiments) guidelines (<https://arriveguidelines.org>), ensuring transparency and reproducibility.

Competing interests

The authors declare no competing interests.

Author details

¹Institute of Marine Biology, National Taiwan Ocean University, Keelung, Taiwan

²Taiwan Ocean Genome Center, National Taiwan Ocean University, Keelung, Taiwan

³Eastern Fishery Research Center, Fisheries Research Institute, Ministry of Agriculture, Taitung, Taiwan

⁴Department of Aquaculture, National Taiwan Ocean University, Keelung, Taiwan

⁵Center of Excellence for the Oceans, National Taiwan Ocean University, Keelung, Taiwan

Received: 9 January 2025 / Accepted: 27 April 2025

Published online: 14 May 2025

References

- Kusakabe K, Hata M, Shoji J, Hori M, Tomiyama T. Effects of water temperature on feeding and growth of juvenile marbled flounder *Pseudopleuronectes yokohamae* under laboratory conditions: evaluation by group-and individual-based methods. *Fish Sci.* 2017;83(2):215–9.
- Kim J-H, Kim SK, Hur YB. Temperature-mediated changes in stress responses, acetylcholinesterase, and immune responses of juvenile Olive flounder *Paralichthys olivaceus* in a bio-floc environment. *Aquaculture.* 2019;506:453–8.
- Hasan MT, Je Jang W, Lee JM, Lee B-J, Hur SW, Gu Lim S, et al. Effects of immunostimulants, prebiotics, probiotics, synbiotics, and potentially immunoreactive feed additives on Olive flounder (*Paralichthys olivaceus*): a review. *Reviews Fisheries Sci Aquaculture.* 2019;27(4):417–37.
- FAO. Fishery and aquaculture statistics. Global aquaculture production 1950–2017 (FishstatJ). FAO fisheries and aquaculture department. 2020.
- Casey P, Zadmajid V, Butts IA, Sørensen SR, Litvak MK. Influence of temperature on growth and survival of juvenile winter flounder, *Pseudopleuronectes americanus* (Walbaum) reared under continuous light. *J World Aquaculture Soc.* 2021;52(1):204–15.
- Islam MJ, Kunzmann A, Slater MJ. Responses of aquaculture fish to climate change-induced extreme temperatures: A review. *J World Aquaculture Soc.* 2022;53(2):314–66.
- Wang Y-B, Li J-R, Lin J. Probiotics in aquaculture: challenges and outlook. *Aquaculture.* 2008;281(1–4):1–4.
- Mraz J, Pickova J. Factors influencing fatty acid composition of common carp (*Cyprinus carpio*) muscle. *Neuroendocrinol Lett.* 2011;32(Suppl 2):3–8.
- Calabretti A, Cateni F, Procida G, Favretto LG. Influence of environmental temperature on composition of lipids in edible flesh of rainbow trout (*Oncorhynchus mykiss*). *J Sci Food Agric.* 2003;83(14):1493–8.
- Skalli A, Robin J, Le Bayon N, Le Delliou H, Person-Le Ruyet J. Impact of essential fatty acid deficiency and temperature on tissues' fatty acid composition of European sea bass (*Dicentrarchus labrax*). *Aquaculture.* 2006;255(1–4):223–32.
- Fraboulet E, Lambert Y, Tremblay R, Audet C. Growth and lipid composition of winter flounder juveniles reared under natural and fixed photoperiod and temperature conditions. *North Am J Aquaculture.* 2011;73(2):89–96.
- Kim KD, Kang YJ, Lee HM, Kim KW, Jang MS, Choi SM, et al. Effects of dietary protein and lipid levels on growth and body composition of subadult Olive flounder, *Paralichthys olivaceus*, at a suboptimal water temperature. *J World Aquaculture Soc.* 2010;41:263–9.
- Ho Y-N, Chen Y-L, Liu D-Y. Portable and rapid sequencing device with microbial Community-Guided culture strategies for precious field and environmental samples. *Msystems.* 2021;6(4):e00748–21.
- Sereika M, Kirkegaard RH, Karst SM, Michaelsen TY, Sørensen EA, Wollenberg RD, et al. Oxford nanopore R10. 4 long-read sequencing enables the generation of near-finished bacterial genomes from pure cultures and metagenomes without short-read or reference polishing. *Nat Methods.* 2022;19(7):823–6.
- Huggins LG, Colella V, Atapattu U, Koehler AV, Traub RJ. Nanopore sequencing using the Full-Length 16S rRNA gene for detection of Blood-Borne Bacteria in dogs reveals a novel species of hemotropic *Mycoplasma*. *Microbiol Spectr.* 2022;10(6):e03088–22.
- Matsuo Y, Komiya S, Yasumizu Y, Yasuoka Y, Mizushima K, Takagi T, et al. Full-length 16S rRNA gene amplicon analysis of human gut microbiota using minion™ nanopore sequencing confers species-level resolution. *BMC Microbiol.* 2021;21:1–13.
- Patti GJ, Yanes O, Siuzdak G. Metabolomics: the apogee of the omics trilogy. *Nat Rev Mol Cell Biol.* 2012;13(4):263–9.
- Samuelsson LM, Larsson DJ. Contributions from metabolomics to fish research. *Mol Biosyst.* 2008;4(10):974–9.
- Samuelsson LM, Björnlén B, Förlin L, Larsson DJ. Reproducible 1H NMR-based metabolomic responses in fish exposed to different sewage effluents in two separate studies. *Environ Sci Technol.* 2011;45(4):1703–10.
- Lardon I, Eyckmans M, Vu TN, Laukens K, De Boeck G, Dommissie R. 1 H-NMR study of the metabolome of a moderately hypoxia-tolerant fish, the common carp (*Cyprinus carpio*). *Metabolomics.* 2013;9:1216–27.
- Kullgren A, Jutfelt F, Fontanillas R, Sundell K, Samuelsson L, Wiklander K, et al. The impact of temperature on the metabolome and endocrine metabolic signals in Atlantic salmon (*Salmo salar*). *Comp Biochem Physiol A: Mol Integr Physiol.* 2013;164(1):44–53.
- De Coster W, D'hert S, Schultz DT, Cruys M, Van Broeckhoven C. Bioinformatics. 2018;34(15):2666–9. NanoPack: visualizing and processing long-read sequencing data.
- Li H. Minimap2: pairwise alignment for nucleotide sequences. *Bioinformatics.* 2018;34(18):3094–100.
- Breitwieser FP, Salzberg SL. Pavian: interactive analysis of metagenomics data for Microbiome studies and pathogen identification. *Bioinformatics.* 2020;36(4):1303–4.
- Xu S, Yu GM. An R package for analysis, visualization and biomarker discovery of Microbiome. *R Package Version.* 2021;1(1).

26. McMurdie PJ, Holmes S. Phyloseq: an R package for reproducible interactive analysis and graphics of Microbiome census data. *PLoS ONE*. 2013;8(4):e61217.
27. Lahti L, Shetty S. microbiome R package. 2017.
28. Wickham H. ggplot2. Wiley interdisciplinary reviews: computational statistics. 2011;3(2):180–5.
29. Asnicar F, Weingart G, Tickle TL, Huttenhower C, Segata N. Compact graphical representation of phylogenetic data and metadata with GraPhlAn. *PeerJ*. 2015;3:e1029.
30. Zhang J, Liu Y-X, Zhang N, Hu B, Jin T, Xu H, et al. NRT1. 1B is associated with root microbiota composition and nitrogen use in field-grown rice. *Nat Biotechnol*. 2019;37(6):676–84.
31. Parks DH, Tyson GW, Hugenholtz P, Beiko RG. STAMP: statistical analysis of taxonomic and functional profiles. *Bioinformatics*. 2014;30(21):3123–4.
32. Soriano B, Hafez AI, Naya-Català F, Moroni F, Moldovan RA, Toxqui-Rodríguez S, et al. SAMBA: Structure-learning of aquaculture microbiomes using a bayesian approach. *Genes*. 2023;14(8):1650.
33. Douglas GM, Maffei VJ, Zaneveld JR, Yurgel SN, Brown JR, Taylor CM, et al. PICRUSt2 for prediction of metagenome functions. *Nat Biotechnol*. 2020;38(6):685–8.
34. Forsberg EM, Huan T, Rinehart D, Benton HP, Warth B, Hilmers B, et al. Data processing, multi-omic pathway mapping, and metabolite activity analysis using XCMS online. *Nat Protoc*. 2018;13(4):633–51.
35. Wang M, Carver JJ, Phelan VV, Sanchez LM, Garg N, Peng Y, et al. Sharing and community curation of mass spectrometry data with global natural products social molecular networking. *Nat Biotechnol*. 2016;34(8):828–37.
36. Metsalu T, Vilo J. *Nucleic Acids Res*. 2015;43(W1):W566–70. ClustVis: a web tool for visualizing clustering of multivariate data using Principal Component Analysis and heatmap.
37. Yu G, Xu C, Zhang D, Ju F, Ni Y, MetOrigin. Discriminating the origins of microbial metabolites for integrative analysis of the gut Microbiome and metabolome. *IMeta*. 2022;1(1):e10.
38. Jang WJ, Hasan MT, Lee B-J, Hur SW, Lee S, Kim KW, et al. Effect of dietary differences on changes of intestinal microbiota and immune-related gene expression in juvenile Olive flounder (*Paralichthys olivaceus*). *Aquaculture*. 2020;527:735442.
39. Sánchez-Cueto P, Stavrakidis-Zachou O, Clos-García M, Bosch M, Papandroulakis N, Lladó S. Mediterranean sea heatwaves jeopardize greater Amberjack's (*Seriola dumeril*) aquaculture productivity through impacts on the fish microbiota. *ISME Commun*. 2023;3(1):36.
40. Zhou C, Gao P, Wang J. Comprehensive analysis of microbiome, metabolome, and transcriptome revealed the mechanisms of intestinal injury in rainbow trout under heat stress. *Int J Mol Sci*. 2023;24(10):8569.
41. Neuman C, Hatje E, Zarkas KZ, Smullen R, Bowman JP, Katouli M. The effect of diet and environmental temperature on the faecal microbiota of farmed T asmanian A Tlantic S Almon (S Almo Salar L). *Aquac Res*. 2016;47(2):660–72.
42. Ley RE, Lozupone CA, Hamady M, Knight R, Gordon JI. Worlds within worlds: evolution of the vertebrate gut microbiota. *Nat Rev Microbiol*. 2008;6(10):776–88.
43. Sepúlveda J, Moeller AH. The effects of temperature on animal gut microbiomes. *Front Microbiol*. 2020;11:512773.
44. Tajima K, Nonaka I, Higuchi K, Takusari N, Kurihara M, Takenaka A, et al. Influence of high temperature and humidity on rumen bacterial diversity in Holstein heifers. *Anaerobe*. 2007;13(2):57–64.
45. Chevalier C, Stojanović O, Colin DJ, Suarez-Zamorano N, Tarallo V, Veyrat-Durebex C, et al. Gut microbiota orchestrates energy homeostasis during cold. *Cell*. 2015;163(6):1360–74.
46. Huyben D, Sun L, Moccia R, Kiessling A, Dicksved J, Lundh T. Dietary live yeast and increased water temperature influence the gut microbiota of rainbow trout. *J Appl Microbiol*. 2018;124(6):1377–92.
47. Niu KM, Lee BJ, Kothari D, Lee WD, Hur SW, Lim SG, et al. Dietary effect of low fish meal Aquafeed on gut microbiota in Olive flounder (*Paralichthys olivaceus*) at different growth stages. *MicrobiologyOpen*. 2020;9(3):e992.
48. Mukhopadhyay I, Hansen R, El-Omar EM, Hold GL. IBD—what role do Proteobacteria play? *Nat Reviews Gastroenterol Hepatol*. 2012;9(4):219–30.
49. Soriano EL, Ramírez DT, Araujo DR, Gómez-Gil B, Castro LI, Sánchez CG. Effect of temperature and dietary lipid proportion on gut microbiota in Yellowtail kingfish *Seriola lalandi* juveniles. *Aquaculture*. 2018;497:269–77.
50. Akhter N, Wu B, Memon AM, Mohsin M. Probiotics and prebiotics associated with aquaculture: a review. *Fish Shellfish Immunol*. 2015;45(2):733–41.
51. Ramírez C, Romero J. Fine flounder (*Paralichthys adspersus*) Microbiome showed important differences between wild and reared specimens. *Front Microbiol*. 2017;8:271.
52. Gauger E, Smolowitz R, Uhlinger K, Casey J, Gómez-Chiarri M. *Vibrio harveyi* and other bacterial pathogens in cultured summer flounder, *Paralichthys dentatus*. *Aquaculture*. 2006;260(1–4):10–20.
53. Shao Y, Zhong H, Mao X, Zhang H. Biochar-immobilized *Sphingomonas* Sp. and *Acinetobacter* Sp. isolates to enhance nutrient removal: potential application in crab aquaculture. *Aquaculture Environ Interact*. 2020;12:251–62.
54. Egerton S, Culloty S, Whooley J, Stanton C, Ross RP. The gut microbiota of marine fish. *Front Microbiol*. 2018;9:873.
55. Niu K-M, Khosravi S, Kothari D, Lee W-D, Lim J-M, Lee B-J, et al. Effects of dietary multi-strain probiotics supplementation in a low fishmeal diet on growth performance, nutrient utilization, proximate composition, immune parameters, and gut microbiota of juvenile Olive flounder (*Paralichthys olivaceus*). *Fish Shellfish Immunol*. 2019;93:258–68.
56. Hu J, You F, Wang Q, Weng S, Liu H, Wang L, et al. Transcriptional responses of Olive flounder (*Paralichthys olivaceus*) to low temperature. *PLoS ONE*. 2014;9(10):e108582.
57. Morowitz MJ, Carlisle EM, Alverdy JC. Contributions of intestinal bacteria to nutrition and metabolism in the critically ill. *Surg Clin*. 2011;91(4):771–85.
58. Metges CC. Contribution of microbial amino acids to amino acid homeostasis of the host. *J Nutr*. 2000;130(7):S1857–64.
59. Henneberry AL, Wright MM, McMaster CR. The major sites of cellular phospholipid synthesis and molecular determinants of fatty acid and lipid head group specificity. *Mol Biol Cell*. 2002;13(9):3148–61.
60. Hazel JR. Thermal adaptation in biological membranes: is homeoviscous adaptation the explanation? *Annu Rev Physiol*. 1995;57(1):19–42.
61. Mejri SC, Tremblay R, Audet C, Wills PS, Riche M. Essential fatty acid requirements in tropical and cold-water marine fish larvae and juveniles. *Front Mar Sci*. 2021:557.
62. Lee S-M, Lee JH, Kim K-D. Effect of dietary essential fatty acids on growth, body composition and blood chemistry of juvenile Starry flounder (*Platichthys stellatus*). *Aquaculture*. 2003;225(1–4):269–81.
63. Furuita H, Takeuchi T, Uematsu K. Effects of eicosapentaenoic and docosahexaenoic acids on growth, survival and brain development of larval Japanese flounder (*Paralichthys olivaceus*). *Aquaculture*. 1998;161(1–4):269–79.
64. Estevez A, Ishikawa M, Kanazawa A. Effects of arachidonic acid on pigmentation and fatty acid composition of Japanese flounder, *Paralichthys olivaceus* (Temminck and Schlegel). *Aquac Res*. 1997;28(4):279–89.
65. Furuita H, Yamamoto T, Shima T, Suzuki N, Takeuchi T. Effect of arachidonic acid levels in broodstock diet on larval and egg quality of Japanese flounder *Paralichthys olivaceus*. *Aquaculture*. 2003;220(1–4):725–35.
66. Tocher DR. Metabolism and functions of lipids and fatty acids in teleost fish. *Rev Fish Sci*. 2003;11(2):107–84.
67. Guschina IA, Harwood JL. Lipids and lipid metabolism in eukaryotic algae. *Prog Lipid Res*. 2006;45(2):160–86.
68. Monroig Ó, Tocher DR, Navarro JC. Biosynthesis of polyunsaturated fatty acids in marine invertebrates: recent advances in molecular mechanisms. *Mar Drugs*. 2013;11(10):3998–4018.
69. Okuyama H, Orikasa Y, Nishida T, Watanabe K, Morita N. Bacterial genes responsible for the biosynthesis of eicosapentaenoic and docosahexaenoic acids and their heterologous expression. *Appl Environ Microbiol*. 2007;73(3):665–70.
70. Zhang J, Sun-Waterhouse D, Su G, Zhao M. New insight into Umami receptor, Umami/umami-enhancing peptides and their derivatives: A review. *Trends Food Sci Technol*. 2019;88:429–38.
71. Ishibashi N, Sadamori K, Yamamoto O, Kanehisa H, Kouge K, Kikuchi E, et al. Bitterness of phenylalanine and tyrosine-containing peptides. *Agric Biol Chem*. 1987;51(12):3309–13.
72. Patel AT, Akhiani RC, Patel MJ, Dedania SR, Patel DH. Bioproduction of L-aspartic acid and cinnamic acid by L-aspartate ammonia lyase from *Pseudomonas aeruginosa* PAO1. *Appl Biochem Biotechnol*. 2017;182:792–803.
73. Arias-Barrau E, Olivera ER, Luengo JM, Fernández C, Galán B, García JL, et al. The homogentisate pathway: a central catabolic pathway involved in the degradation of L-phenylalanine, L-tyrosine, and 3-hydroxyphenylacetate in *Pseudomonas putida*. *J Bacteriol*. 2004;186(15):5062–77.
74. Flieger A, Gong S, Faigle M, Deeg M, Bartmann P, Neumeister B. Novel phospholipase A activity secreted by *Legionella* species. *J Bacteriol*. 2000;182(5):1321–7.
75. Fürch T, Preusse M, Tomasch J, Zech H, Wagner-Döbler I, Rabus R, et al. Metabolic fluxes in the central carbon metabolism of *Dinoroseobacter shibae* and

Phaeobacter gallaeciensis, two members of the marine Roseobacter clade. *BMC Microbiol.* 2009;9:1–11.

76. Nichols DS, Nichols PD, McMeekin TA. Polyunsaturated fatty acids in Antarctic bacteria. *Antarct Sci.* 1993;5(2):149–60.
77. Na H, Jo S-W, Do J-M, Kim I-S, Yoon H-S. Production of algal biomass and high-value compounds mediated by interaction of microalgal *Oocystis* Sp. KNUA044 and bacterium *Sphingomonas* KNU100. *J Microbiol Biotechnol.* 2021;31(3):387.

Publisher's note

Springer Nature remains neutral with regard to jurisdictional claims in published maps and institutional affiliations.